



# Increased Resistance to Intradermal *Francisella tularensis* LVS Infection by Inactivation of the Sts Phosphatases

Kaustubh Parashar,<sup>a</sup> Erik Kopping,<sup>a,c</sup> David Frank,<sup>a,b</sup> Vinaya Sampath,<sup>a,c</sup>  
David G. Thanassi,<sup>a,c</sup> Nick Carpino<sup>a</sup>

Department of Molecular Genetics and Microbiology, Stony Brook University, Stony Brook, New York, USA<sup>a</sup>;  
Graduate Program in Molecular and Cellular Pharmacology, Stony Brook University, Stony Brook, New York,  
USA<sup>b</sup>; Center for Infectious Diseases, Stony Brook University, Stony Brook, New York, USA<sup>c</sup>

**ABSTRACT** The Suppressor of ICR signaling proteins (Sts-1 and Sts-2) are two homologous phosphatases that negatively regulate signaling pathways in a number of hematopoietic lineages, including T lymphocytes. Mice lacking Sts expression are characterized by enhanced T cell responses. Additionally, a recent study demonstrated that *Sts*<sup>-/-</sup> mice are profoundly resistant to systemic infection by *Candida albicans*, with resistance characterized by enhanced survival, more rapid fungal clearance in key peripheral organs, and an altered inflammatory response. To investigate the role of Sts in the primary host response to infection by a bacterial pathogen, we evaluated the response of *Sts*<sup>-/-</sup> mice to infection by a Gram-negative bacterial pathogen. *Francisella tularensis* is a facultative bacterial pathogen that replicates intracellularly within a variety of cell types and is the causative agent of tularemia. *Francisella* infections are characterized by a delayed immune response, followed by an intense inflammatory reaction that causes widespread tissue damage and septic shock. Herein, we demonstrate that mice lacking Sts expression are significantly resistant to infection by the live vaccine strain (LVS) of *F. tularensis*. Resistance is characterized by reduced lethality following high-dose intradermal infection, an altered cytokine response in the spleen, and enhanced bacterial clearance in multiple peripheral organs. *Sts*<sup>-/-</sup> bone marrow-derived monocytes and neutrophils, infected with *F. tularensis* LVS *ex vivo*, display enhanced restriction of intracellular bacteria. These observations suggest the Sts proteins play an important regulatory role in the host response to bacterial infection, and they underscore a role for Sts in regulating functionally relevant immune response pathways.

**KEYWORDS** *Francisella*, host resistance, host-pathogen interactions

**F***Francisella tularensis* is a Gram-negative, facultative intracellular bacterial pathogen. It is the causative agent of tularemia or rabbit fever and remains one of the most infectious bacterial pathogens known to man. Inhalation of as few as 10 bacterial CFU is sufficient to initiate an infection in humans (1). Therefore, the Centers for Disease Control and Prevention has classified *Francisella tularensis* as a category A bioterrorism agent (2). The symptoms of tularemia are dependent on the route of infection—transmission can be ulceroglandular (e.g., through tick bites), oculoglandular (through conjunctiva), oropharyngeal (through consumption of contaminated meat), or pneumonic (through inhalation) (3). The patient usually presents with flu-like symptoms with enlarged lymph nodes. Additionally, patients with respiratory tularemia have congestion and impaired breathing. If left untreated, the fatality rate can be as high as 50 to 60% (4). Studies involving *Francisella* are the subject of significant interest due to *Francisella*'s potential role as an agent of bioterrorism and because the bacterium

Received 5 June 2017 Accepted 6 June 2017

Accepted manuscript posted online 19 June 2017

**Citation** Parashar K, Kopping E, Frank D, Sampath V, Thanassi DG, Carpino N. 2017. Increased resistance to intradermal *Francisella tularensis* LVS infection by inactivation of the Sts phosphatases. *Infect Immun* 85:e00406-17. <https://doi.org/10.1128/IAI.00406-17>.

**Editor** Andreas J. Bäuml, University of California, Davis

**Copyright** © 2017 American Society for Microbiology. All Rights Reserved.

Address correspondence to Nick Carpino, [nicholas.carpino@stonybrook.edu](mailto:nicholas.carpino@stonybrook.edu).

serves as an excellent model pathogen to study host responses with respect to an intracellular bacterial pathogen (5, 6).

*Francisella tularensis* has two clinically relevant subspecies (*F. tularensis* subsp. *tularensis* and *F. tularensis* subsp. *holarctica*), each differing in geographical location and pathogenicity (5). The *F. tularensis* live vaccine strain (LVS) is derived from *F. tularensis* subsp. *holarctica* via repeated passage on agar and in animals (7). It is nonpathogenic in humans, but infection by LVS mimics the clinical symptoms of tularemia in mice. Thus, it can be useful in studying *Francisella's* mechanisms of pathogenicity and host immune responses. Following a lethal infectious dose, the bacteria spread to organs of the reticuloendothelial system (spleen, liver, and lung) regardless of the route of infection and reaches peak bacterial load within 3 to 4 days (8). Large-scale myeloid cell infiltration in response to the infection and consequent necrotic tissue damage worsen the pathology (9). Death by septicemia is usually observed within 8 days of infection in moribund mice. However, mice receiving sublethal dosages are able to clear out the bacteria within a span of 2 to 4 weeks postinfection.

In recent years, the intracellular life cycle of *Francisella*, bacterial pathogenicity mechanisms, and host inflammatory responses to *Francisella* infection have been the subject of intense study (10–12). After phagocytosis into host cells following interactions with either the complement receptor CR3, mannose receptors, class A scavenger receptors, or  $Fc\gamma$  receptors, *Francisella* enters into a vacuolar compartment known as the *Francisella*-containing phagosome (FCP) (13). It then rapidly escapes from the phagosome prior to phagolysosomal fusion and enters the cytoplasm (10). Within the cytoplasm, it replicates to high numbers while suppressing host apoptotic and inflammatory response pathways (13–15). The DNA-sensing inflammasome component AIM2 has been identified as a critical mediator of inflammasome activation and cell death (16, 17). Interestingly, it has recently been shown that with regard to *Francisella novicida*, bacterial DNA from lysed or rapidly replicating cells within the host cytosol is detected by the cytosolic sensor cGAS-STING, leading to activation of a type-1 interferon-dependent signaling cascade that activates guanylate-binding proteins (GBPs) and IRGB10 (18). Binding of GBPs and IRGB10 to the bacterial surface leads to bacterial lysis and further release of bacterial lysis products into the host cytoplasm. This initiates host AIM2 or NLRP3 inflammasome activation, resulting in caspase-dependent cell death (19). Cell death at early time points postinfection is thought to limit bacterial spread and therefore is considered an important host defense mechanism.

Two homologous phosphatases, Sts-1 and Sts-2, have been established as negative regulators of signaling pathways within cells of the mammalian immune system, most prominently T cells. The Sts proteins are characterized by a distinct tripartite structure consisting of two protein-interaction domains and a C-terminal 2H-phosphatase domain. They are structurally and enzymatically very distinct from other intracellular phosphatases that regulate immune signaling pathways (20). The two Sts proteins are more than 50% identical at the amino acid level and have been shown to have overlapping, if not redundant, signaling functions. However, while Sts-1 expression appears to be ubiquitous, Sts-2 expression is more limited and is confined primarily to cells of hematopoietic origin (21). Of the two, Sts-1 is the more active enzyme *in vitro*. While the Sts proteins were initially described as regulators of T cell signaling due to their ability to target the critical T cell kinase Zap-70, recent evidence has uncovered a broader role for the Sts proteins in regulating additional cellular pathways within mast cells and platelets (22, 23). Mice lacking Sts-1 and Sts-2 (*Sts*<sup>-/-</sup>) have no overt phenotypic disorders, although some immune cells derived from *Sts*<sup>-/-</sup> mice show heightened responsiveness *in vitro* (21, 24).

The role of the Sts proteins in regulating host-pathogen interactions is an area of active interest that has just begun to be explored. Recently, *Sts*<sup>-/-</sup> mice were evaluated for susceptibility to infection by the important human fungal pathogen *Candida albicans*, using a mouse model that mimics systemic candidiasis in humans (25). Unlike wild-type mice, in which rapid fungal proliferation in peripheral organs leads to progressive sepsis and rapid lethality, *Sts*<sup>-/-</sup> mice exhibit a profound resistance to

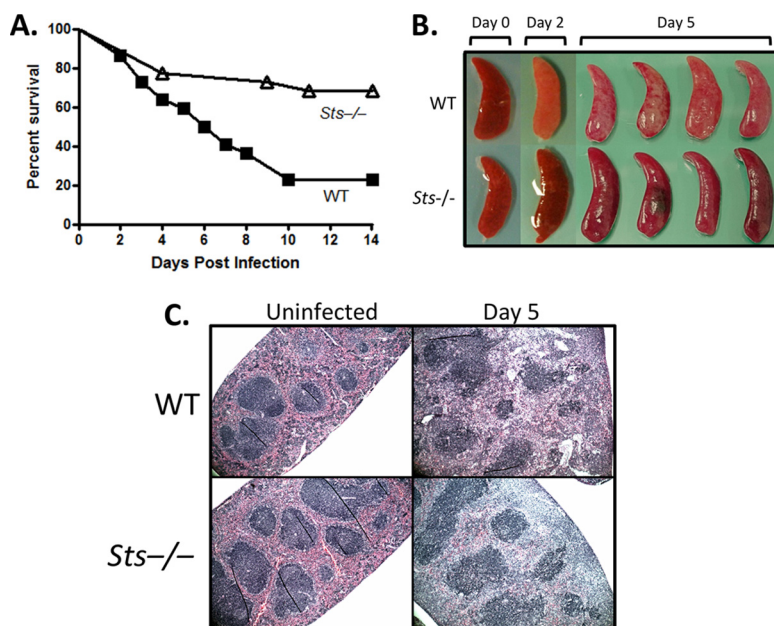


**FIG 1** Survival advantage and reduced tissue pathology of *Sts*<sup>-/-</sup> mice. (A) Mice were infected intradermally with a lethal dose [(4.4 ± 0.5) × 10<sup>7</sup>] of *Francisella tularensis* LVS bacteria and monitored for a total of 28 days. *Sts*<sup>-/-</sup> mice demonstrated significantly enhanced survival ( $P = 0.00018$  by log rank test). A cumulative total of 22 mice per genotype were evaluated, in three independent experiments. (B) In contrast to wild-type spleens, *Sts*<sup>-/-</sup> spleens do not display extensive signs of necrotic damage following *F. tularensis* infection. Spleens were removed from infected animals on the indicated day postinfection. (C) Representative histological analysis of wild-type and *Sts*<sup>-/-</sup> spleens 5 days after lethal LVS intradermal infection. Staining was with H&E. Magnification, ×40. WT, wild type.

infection (25). Importantly, the *Sts*<sup>-/-</sup> response is associated with a significant reduction in fungal burden in critical target organs, sharply diminished levels of many inflammatory molecules beginning at 24 h postinfection, and an absence of inflammatory lesions. Thus, current evidence suggests that *Sts* inactivation results in a distinct immune response that is uniquely capable of restricting a deadly human fungal pathogen. To further our understanding of the broader role the *Sts* proteins in host-pathogen interactions, we evaluated the response of *Sts*<sup>-/-</sup> mice to *F. tularensis* LVS infection. Our results demonstrate that genetic inactivation of the *Sts* proteins leads to significantly increased resistance to intradermal *F. tularensis* LVS challenge. Notably, bone marrow-derived monocytes (BMD-mo) and neutrophils isolated from bone marrow and lacking *Sts* expression display enhanced bactericidal activity *ex vivo* relative to wild-type cells. These results highlight an important role for *Sts*-1 and *Sts*-2 in regulating host responses to bacterial pathogens.

## RESULTS

***Sts*<sup>-/-</sup> mice are protected from lethal *F. tularensis* LVS infection.** The role of *Sts*-1 and *Sts*-2 in regulating the host response to a bacterial pathogen was examined by evaluating the susceptibility of *Sts*<sup>-/-</sup> mice to systemic infection by *F. tularensis* LVS. After a period of active immune suppression by *Francisella* during the early stages of LVS infection, excessive inflammatory responses triggered during the latter stages of lethal infection exacerbate the course of disease and lead to detrimental pathological outcomes, including progressive sepsis and multiorgan failure (26). Mice were inoculated via intradermal injections [(4.4 ± 0.5) × 10<sup>7</sup> CFU/mouse], and then the animals were monitored over a 28-day period. As expected, more than 50% of wild-type mice became moribund within the first week following infection, and by the end of 14 days, only 25% remained alive (Fig. 1A). In contrast, mice lacking the *Sts* proteins exhibited strikingly enhanced survival following infection. Specifically, of the infected *Sts*<sup>-/-</sup> mice, only 30% became moribund by 14 days (Fig. 1A). These results demonstrate that

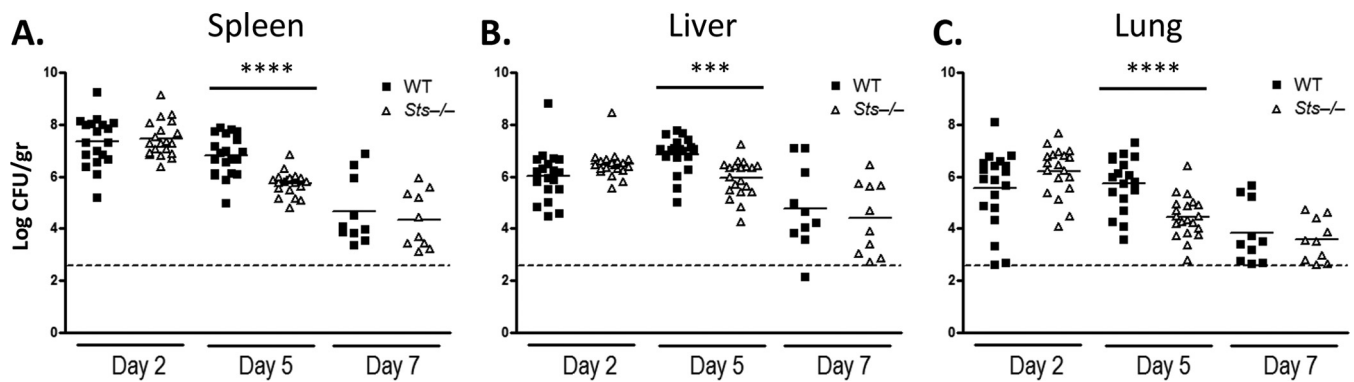


**FIG 2** Accelerated bacterial clearance in peripheral organs of *Sts*<sup>-/-</sup> mice. Bacterial burdens in the spleen (A), liver (B), and lungs (C) at 2, 5, and 7 days postinfection with an inoculum of  $(2.52 \pm 1.16) \times 10^7$  CFU/mouse. Cumulative data were compiled from four separate experiments with five mice per group. \*\*\*,  $P < 0.001$ ; \*\*\*\*,  $P < 0.0001$  (by standard *t* test).

mice lacking *Sts*-1 and *Sts*-2 expression are protected from lethal intradermal infection by *F. tularensis* LVS. Survival studies performed with both higher and lower infectious doses yielded similar results (see Fig. S1A and B in the supplemental material). However, in contrast to the enhanced survival of *Sts*<sup>-/-</sup> animals following intradermal infection, *Sts* inactivation did not lead to enhanced survival following intranasal inoculation of *F. tularensis* LVS (Fig. S1C).

Over the early course of a lethal LVS infection, peripheral organs such as the spleen develop severe inflammation and extensive necrosis (27). To determine whether or not expected pathogenic effects were present following *Francisella* LVS infection of *Sts*<sup>-/-</sup> mice, we examined the spleens of infected mice. Whereas spleens from wild-type and *Sts*<sup>-/-</sup> mice were indistinguishable prior to infection, spleens isolated from infected mice were noticeably different in gross appearance, with differences becoming apparent by day 2 postinfection (p.i.) (Fig. 1B). Spleens dissected from wild-type mice on day 5 p.i. appeared uniformly pale in color due to the development of necrotic lesions (27) (Fig. 1B, top). In contrast, spleens from *Sts*<sup>-/-</sup> mice on day 5 p.i. appeared enlarged but otherwise healthy (Fig. 1B, bottom). Histological analysis of wild-type and *Sts*<sup>-/-</sup> spleens on day 5 p.i. revealed noticeable differences in splenic architecture. In particular, while the internal structure of wild-type spleens was significantly disrupted, spleens obtained from mutant animals displayed distinct areas of white and red pulp and retention of marginal zone areas (Fig. 1C). These results support the notion that *Sts*<sup>-/-</sup> mice have increased resistance to lethal *Francisella* infection relative to wild-type mice and suggest that the widespread organ damage that accompanies *F. tularensis* infection is less pervasive in the absence of *Sts* protein expression.

**Accelerated bacterial clearance in *Sts*<sup>-/-</sup> peripheral organs.** The enhanced survival of *Sts*<sup>-/-</sup> mice following lethal *F. tularensis* challenge and lack of overt splenic pathology suggests that mice lacking *Sts* expression were better at either tolerating a higher splenic bacterial burden or disabling pathogen virulence mechanisms and clearing the infection, or a combination of both. To determine how bacterial burden was controlled within spleens of *Sts*<sup>-/-</sup> mice, we infected animals by intradermal inoculation [ $(2.52 \pm 1.16) \times 10^7$  CFU/mouse] and assessed the bacterial load on days 2, 5, and 7 following infection. On day 2, both wild-type and *Sts*<sup>-/-</sup> mice contained similarly high counts of splenic CFU (Fig. 2A). This suggests that during the first 2 days following infection, rapid bacterial growth and widespread dissemination occur similarly in wild-type and *Sts*<sup>-/-</sup> hosts. However, by day 5, as the infection was cleared following mobilization of the host innate immune response, the bacterial load in *Sts*<sup>-/-</sup> mouse spleens was consistently 10-fold lower than in wild-type spleens (Fig. 2A). Continued bacterial clearance up to day 7 was observed in wild-type and *Sts*<sup>-/-</sup> spleens, with a trend toward lower counts of bacterial CFU in day 7 mutant mouse spleens. In addition to the spleen, the liver and lung are two other reticuloendothelial organs that are sites of acute bacterial replication following intradermal infection (26).

**TABLE 1** Summary of cellular infiltrates into peripheral organs<sup>a</sup>

Organ	Cell infiltrate	% of cells in mice					
		Day 0		Day 2		Day 5	
		WT	<i>Sts</i> <sup>-/-</sup>	WT	<i>Sts</i> <sup>-/-</sup>	WT	<i>Sts</i> <sup>-/-</sup>
Spleen	CD11b <sup>+</sup>	15.5 ± 3.05	14.8 ± 5.56	17.3 ± 4.88	19.3 ± 5.34	16.8 ± 4.92	25 ± 7.20
	Mono/Mac	20 ± 5.5	23.8 ± 3.33	1.81 ± 1.77	3.18 ± 2.18	21.1 ± 3.44	12.6 ± 1.59
	Neutrophil	34.8 ± 4.55	35.4 ± 7.61	47.6 ± 8.62	43.1 ± 5.53	46.9 ± 8.56	60.4 ± 5.06*
	NK cells	16.1 ± 3.24	17.2 ± 2.7	3.22 ± 1.9	3.54 ± 2.18	6.74 ± 2.00	4.87 ± 2.42
	B cells	50.6 ± 5.01	52.2 ± 6.8	51.3 ± 8.60	50.6 ± 9.98	50.9 ± 7.07	48.9 ± 6.84
	T cells	26.4 ± 2.84	27.3 ± 3.87	23.0 ± 2.10	19.1 ± 3.94	25.3 ± 1.94	18.0 ± 2.71
Liver	CD11b <sup>+</sup>	31 ± 4.13	31.5 ± 2.02	45.6 ± 15.3	61.3 ± 1.65	79.6 ± 6.87	75.4 ± 4.70
	Mono/Mac	22.3 ± 7.62	30.7 ± 1.48	6.25 ± 6.98	6.15 ± 3.08	24.5 ± 8.19	23.5 ± 2.95
	Neutrophil	40.7 ± 14.2	40.3 ± 4.7	39.3 ± 9.71	49.6 ± 5.08*	47.9 ± 7.25	48.5 ± 4.46
	NK cells	22.6 ± 4.02	19.5 ± 0.40	26.5 ± 17.3	13.6 ± 2.51	14.9 ± 3.73	12.5 ± 3.51
	B cells	27.0 ± 2.50	36.0 ± 3.47	20.3 ± 5.81	13.4 ± 1.57	6.3 ± 5.14	9.44 ± 3.27
	T cells	33.8 ± 2.25	25.9 ± 2.37	23.7 ± 6.24	24.0 ± 7.98	30.8 ± 6.71	28.2 ± 4
Lung	CD11b <sup>+</sup>	30.7 ± 3.79	30.2 ± 3.07	56.5 ± 8.70	59.5 ± 5.17	77.7 ± 5.45	76.2 ± 9.56
	Mono/Mac	39.8 ± 5.47	38.2 ± 11.5	25.0 ± 6.16	23.0 ± 6.13	16.4 ± 4.02	17.2 ± 6.48
	Neutrophil	20.6 ± 4.84	21.8 ± 2.86	26.8 ± 9.82	28.6 ± 7.96	29.1 ± 9.51	29.6 ± 7.44
	NK cells	23.0 ± 7.22	17.7 ± 3.01	19.3 ± 4.76	16.0 ± 6.02	19.9 ± 7.18	13.8 ± 6.89
	B cells	37.0 ± 4.39	47.5 ± 2.99	26.0 ± 8.25	26.7 ± 2.62	15.6 ± 2.02	17.2 ± 6.03
	T cells	18.7 ± 1.89	16.9 ± 2.55	22.5 ± 3.46	22 ± 3.55	8.37 ± 3.03	14.4 ± 13.9

<sup>a</sup>Summary of organ-specific cellular infiltrates following lethal *F. tularensis* LVS infection of wild-type (WT) or *Sts*<sup>-/-</sup> mice. Values are percentages of cells in the total 7-aminoactinomycin D-negative (7AAD<sup>-</sup>) population (live cells, spleen) or 7AAD<sup>-</sup>/CD45<sup>+</sup> live cell gate (liver/lungs), with cells defined as monocytes/macrophages (Mono/Mac) (CD11b<sup>+</sup> CD115<sup>+</sup>), neutrophils (CD11b<sup>+</sup> Ly6G<sup>+</sup>), NK cells (NK1.1<sup>+</sup>), B cells (CD19<sup>+</sup>), or T cells (CD3<sup>+</sup>).

Within these two organs, enhanced bacterial clearance by days 5 and 7 was also evident in *Sts*<sup>-/-</sup> mice relative to wild-type mice (Fig. 2B and C). Thus, in diverse peripheral organs, mice lacking the Sts proteins eliminate the infection at a higher rate than wild-type mice.

**Altered inflammatory environment within *Sts*<sup>-/-</sup> spleens.** During the early stages of primary severe *Francisella* infection, innate leukocyte recruitment into infected tissues crucially influences the outcome of disease (9, 28). For example, in a pulmonary infection model, it has been shown that a lethal infectious dose stimulates immature myeloid cell and myeloid-derived suppressor cell (MDSC) infiltration into the lungs. Cell recruitment into the lungs, followed by their premature death, is associated with increased host tissue damage, leading to a deleterious outcome (9). In contrast, a sublethal dose drives a predominantly neutrophil/mature monocyte response, resulting in a more protective outcome (9). The enhanced survival and accelerated bacterial clearance evident in *Sts*<sup>-/-</sup> spleens relative to wild-type spleens following challenge with a lethal dose of *Francisella* suggest potential differences in cell recruitment into the spleen. Therefore, we examined the influx of leukocytes into spleens of wild-type and *Sts*-1/2<sup>-/-</sup> mice over a 0- to 5-day time course. Splenic myeloid and lymphoid cell populations were enumerated at 2 and 5 days p.i. No significant differences were seen in the numbers of lymphocytes, macrophages, monocytes, NK cells, and dendritic cells (DCs) infiltrating into the spleen over a time course of infection (Table 1). We also did not observe significant differences in the levels of cellular recruitment into lungs and liver (Table 1). However, significant differences were observed in the level of recruitment of neutrophils into the spleens and livers of *Sts*<sup>-/-</sup> mice. Specifically, *Sts*<sup>-/-</sup> spleens presented with increased neutrophil infiltration as a percentage of total leukocytes 5 days p.i. relative to wild-type mice (Fig. 3A and B), while increased levels of neutrophils within *Sts*<sup>-/-</sup> mouse livers were observed on day 2 postinfection (Fig. 3A and C). No significant difference in neutrophil infiltration into lungs during days 0 to 5 p.i. was observed (Fig. 3A and D). Thus, within spleens and livers, increased neutrophil recruitment was associated with decreased counts of bacterial CFU. Given that lung tissue did not display increased levels of neutrophils, however, it is not clear if the two responses are causally related. Interestingly, in contrast to what is observed during

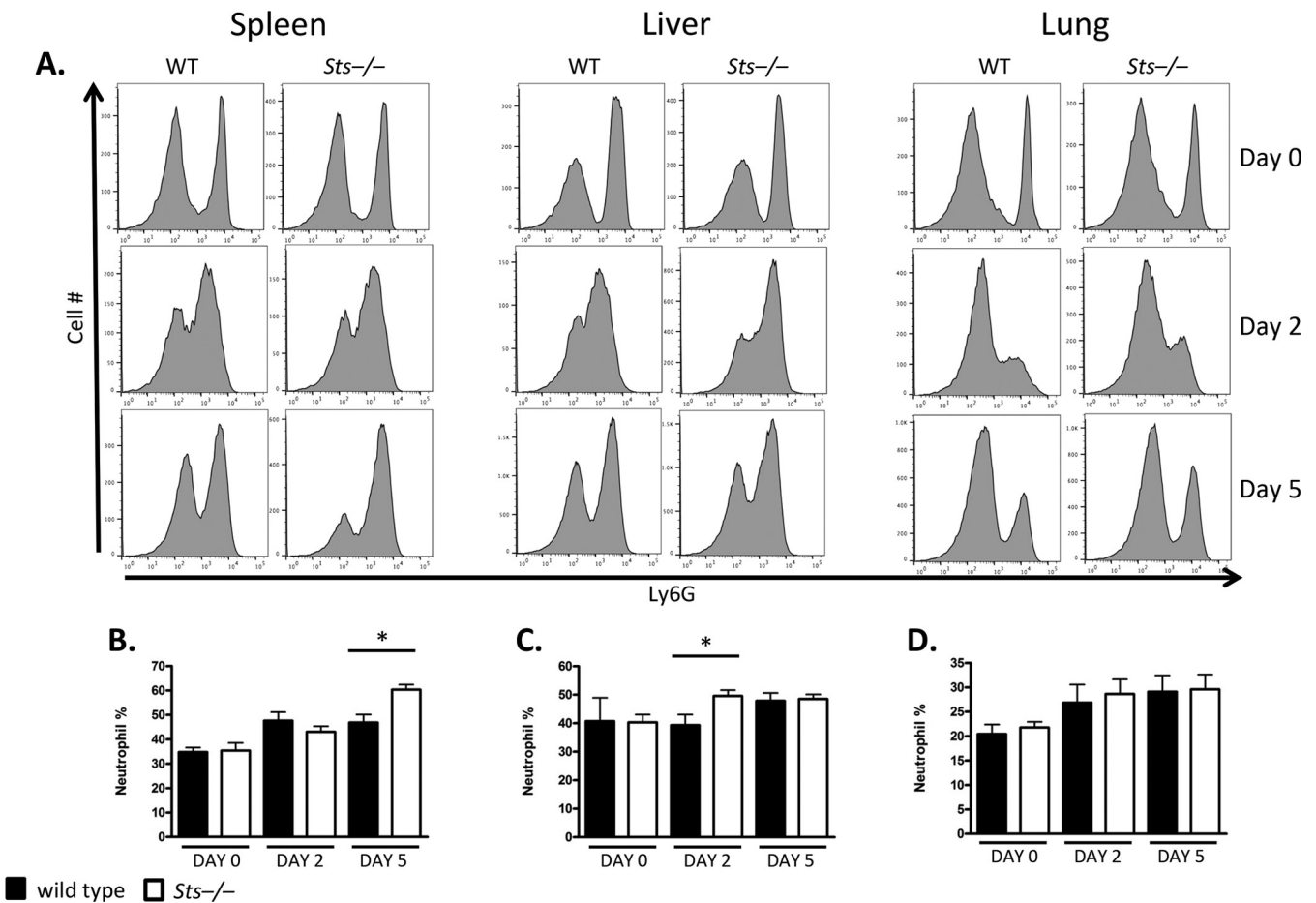


**FIG 3** Alterations in neutrophil recruitment into the spleen and liver in infected *Sts*<sup>-/-</sup> mice. (A) Representative fluorescence-activated cell sorter histogram plots illustrating changes in the levels of CD11b<sup>+</sup> Ly6G<sup>+</sup> neutrophils within peripheral organs following lethal *F. tularensis* LVS infection. A summary of fluorescence-activated cell sorter plots, with the total flow cytometric data from two independent experiments (three mice per group), for the spleen (B), liver (C), and lung (D) is shown. \*,  $P < 0.05$  (by standard  $t$  test).

infection of *Sts*<sup>-/-</sup> hosts, excessive neutrophil influx into lung tissue following *F. tularensis* pulmonary infection of wild-type mice is correlated with a dysregulated immune response that is deleterious to the host (29, 30).

We then further investigated the inflammatory environment of infected spleens from wild-type and *Sts*<sup>-/-</sup> mice by evaluating levels of pro- and antiinflammatory cytokines over a time course of infection. As part of its virulence strategy, *Francisella* is thought to manipulate expression of pro- and antiinflammatory cytokines within the host. Tumor necrosis factor alpha (TNF- $\alpha$ ), gamma interferon (IFN- $\gamma$ ), and interleukin 6 (IL-6) are critical proinflammatory cytokines that are upregulated within infected macrophages and DCs following interaction of *Francisella* lipoproteins with TLR2 (13). While the levels of these three cytokines within spleens of infected mice changed significantly as part of a "cytokine storm" during the first 5 days p.i., there were no differences in cytokine expression levels between wild-type and *Sts*<sup>-/-</sup> spleens (Fig. 4A). In contrast, proinflammatory IL12p70, which is also produced by macrophages and DCs, was significantly upregulated in infected *Sts*<sup>-/-</sup> spleens on day 2 relative to wild-type spleens on day 2 (Fig. 4B), despite each organ having similar numbers of CFU at that time point. We also detected an increased expression of proinflammatory IL-15 and IL-17 in infected *Sts*<sup>-/-</sup> spleens on day 2 relative to that in wild-type spleens on day 2 (Fig. 4B). Furthermore, infected *Sts*<sup>-/-</sup> spleens on day 2 also expressed significantly greater levels of antiinflammatory cytokines IL-4, IL-10, and IL-13 than infected wild-type spleens on day 2 (Fig. 4C). These results suggest the *Sts* proteins negatively regulate a subset of critical inflammatory responses during the initial stages of primary

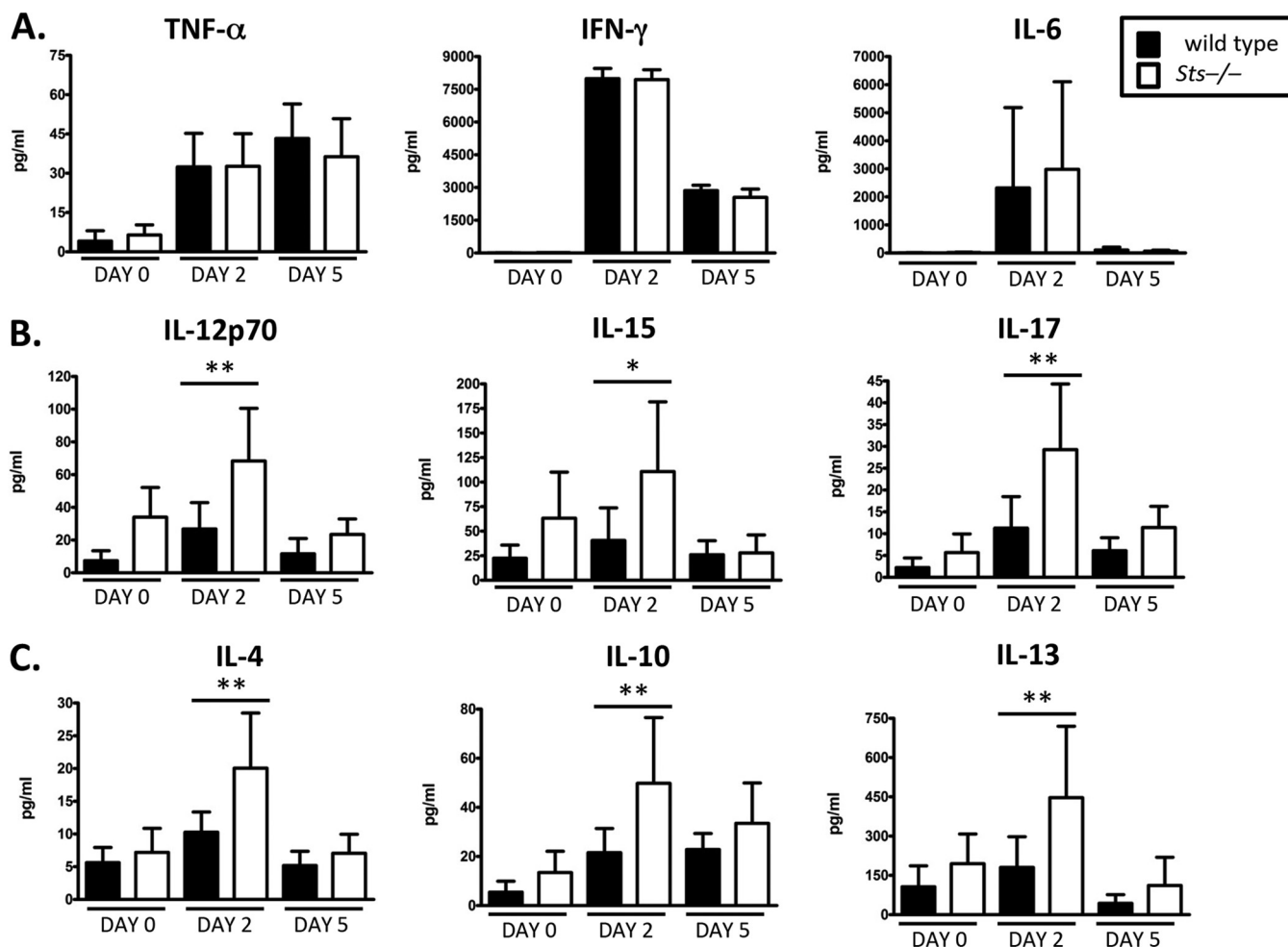


**FIG 4** Altered splenic cytokine environment in the absence of *Sts* expression. Mice were infected with a lethal infectious dose of *F. tularensis* LVS [(4.4  $\pm$  0.5)  $\times$  10<sup>7</sup> CFU/mouse], and spleens were harvested at the indicated time points and analyzed. (A) Levels of the inflammatory cytokines TNF- $\alpha$ , IFN- $\gamma$ , and IL-6 within the spleen were determined by a multiplex assay. The results of two independent experiments (three mice per group) are displayed. (B) Levels of the proinflammatory cytokines IL-12p70, IL-15, and IL-17 within the spleen were determined by a multiplex assay. The results of two independent experiments (three mice per group) are displayed. (C) Levels of the antiinflammatory cytokines IL-4, IL-10, and IL-13 within the spleen were determined by a multiplex assay. The results of two independent experiments (three mice per group) are displayed. \*,  $P < 0.05$ ; \*\*,  $P < 0.01$  (by Mann-Whitney analysis).

bacterial infection in a nonspecific manner, as evidenced by the increased levels of both proinflammatory and antiinflammatory cytokines.

***Sts* proteins regulate innate leukocyte bactericidal effector functions.** Following uptake into macrophages, *Francisella* blocks cell-autonomous antibacterial responses, escapes the phagosome, and replicates to high titers in the cytosol (31). The ability to survive and replicate within macrophages is considered an important pathogenicity mechanism that allows for rapid bacterial spread within a host (32). To determine whether the *Sts* proteins regulate the ability of *Francisella* to replicate within macrophages, we performed *ex vivo* infection assays. We observed no differences in 24-h bacterial growth in *ex vivo* cultures of wild-type and *Sts*<sup>-/-</sup> bone marrow-derived macrophages (BMDM) (Fig. 5A), a result that is not inconsistent with equivalent bacterial CFU levels in peripheral organs of wild-type and *Sts*<sup>-/-</sup> mice by day 2 p.i. However, the accelerated bacterial clearance evident in *Sts*<sup>-/-</sup> tissues suggested that *Sts*<sup>-/-</sup> tissue leukocytes possess enhanced microbicidal properties. To further investigate potential underlying cellular causes, we evaluated the ability of monocytes to restrict bacterial growth. Bone marrow-derived monocytes (BMD-mo), obtained by the method of Francke et al. (33) and phenotypically distinct from BMDMs (see Fig. S3 in the supplemental material), were either left untreated or treated with phorbol myristate

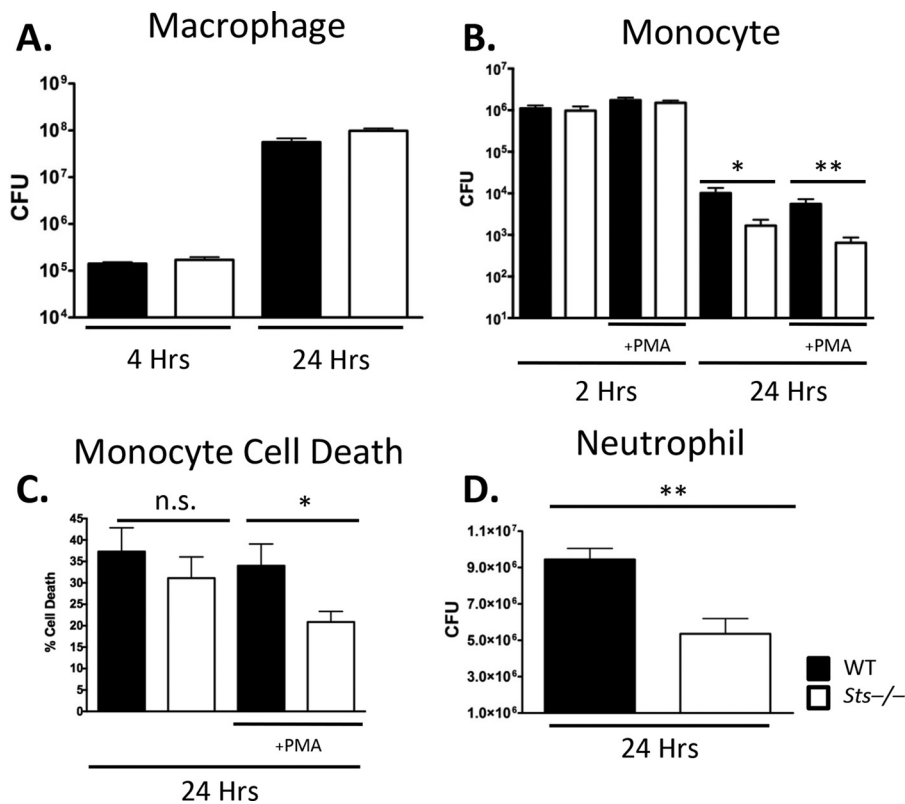


**FIG 5** Enhanced bactericidal properties of *Sts*<sup>-/-</sup> leukocytes. (A) Loss of *Sts* does not affect the intracellular growth of *F. tularensis* in macrophages. Bone marrow-derived macrophages were infected with *F. tularensis* LVS (MOI, 50) for 2 h, extracellular bacteria were eliminated by gentamicin treatment, and cells were incubated for an additional 24 h. Cells were then lysed, and the bacterial CFU were enumerated. Data are from three separate experiments, each performed in triplicate. (B) Enhanced restriction of LVS within *Sts*<sup>-/-</sup> bone marrow-derived monocytes. Monocytes received a 2-h pretreatment with PMA as specified prior to infection (MOI, 5), extracellular bacteria were eliminated by gentamicin treatment after 2 h, and cells were incubated for an additional 24 h. Cells were then lysed, and the bacterial CFU were enumerated. Cumulative data from three separate experiments, each performed in quadruplicate, are displayed. (C) Decreased bacterially induced cytotoxicity within *Sts*<sup>-/-</sup> monocytes. Bone marrow-derived monocytes were infected with *F. tularensis* LVS as described above. After 24 h, culture supernatants were collected and cytotoxicity was quantified by measuring LDH release by a colorimetric assay. Cumulative data were compiled from three separate experiments, each performed in triplicate. (D) Enhanced restriction of LVS within *Sts*<sup>-/-</sup> neutrophils. Neutrophils isolated from murine bone marrow and treated with PMA were infected with *F. tularensis* LVS (MOI, 5). After 24 h, cells were lysed and the numbers of bacterial CFU in the cultures were determined. Data are compiled from three separate experiments, each performed in triplicate. \*,  $P < 0.05$ ; \*\*,  $P < 0.01$ .

acetate (PMA) to heighten their activation state. We observed similar levels of bacterial internalization in wild-type and *Sts*<sup>-/-</sup> marrow-derived monocyte cultures (Fig. 5B, 2 h). In contrast to BMDMs, marrow-derived monocytes are able to restrict intracellular *Francisella* growth (Fig. 5B). Interestingly, we observed a 10-fold-greater restriction of intracellular *Francisella* bacteria by *Sts*<sup>-/-</sup> monocytes than by wild-type monocytes following 24 h of *ex vivo* culture, regardless of PMA treatment (Fig. 5B, 24 h). The enhanced bactericidal activity of *Sts*<sup>-/-</sup> monocytes was also accompanied by significantly reduced cellular cytotoxicity, as observed in the PMA-treated samples (Fig. 5C). Because neutrophils are also among the leukocyte populations recruited to local sites of infection, and *Francisella* has been demonstrated to infect neutrophils and impair their intrinsic microbicidal effector functions (34, 35), we assessed the ability of wild-type and *Sts*<sup>-/-</sup> bone marrow neutrophils to restrict *Francisella* in *ex vivo* coculture. As with bone marrow-derived monocytes, we noted an enhanced intracellular restriction of *Francisella* by *Sts*<sup>-/-</sup> neutrophils relative to wild-type neutrophils, although the effects of *Sts* inactivation in neutrophils were not as great as those observed in monocytes (Fig. 5D). Bone marrow-derived monocytes were also assessed for their



ability to restrict a clinically isolated virulent strain of *Francisella*, *F. tularensis* subsp. *holarctica* KY99-3387. Monocytes received a 2-h treatment of IFN- $\gamma$ /PMA prior to infection in order to enhance bactericidal responses. A clear trend showing greater restriction of the pathogen by *Sts*<sup>-/-</sup> monocytes across all the three individual experiments was observed (Fig. S2).

## DISCUSSION

This study broadens our understanding of host-pathogen interactions and the molecular mechanisms that control primary host immune responses toward microbial pathogens. Here, we demonstrate a role for Sts-1 and Sts-2 in regulating the primary immune response to intradermal infection by a highly virulent Gram-negative bacterial pathogen. In particular, mice lacking Sts expression are shown to be significantly resistant to infection by *F. tularensis* LVS. The resistance of *Sts*<sup>-/-</sup> mice is characterized by increased survival following a lethal infectious dose, altered levels of inflammatory cytokine expression in the periphery shortly after infection, reduced organ-specific pathology, and enhanced bacterial clearance in multiple organs. To our knowledge, this is the first demonstration that the Sts proteins play a role in regulating the host response to a bacterial infection, and it underscores a role for Sts in controlling functionally relevant innate immune response pathways.

The Sts proteins are a pair of homologous enzymes belonging to the histidine phosphatase superfamily of enzymes, so-called because family members contain an evolutionarily conserved histidine residue that functions as a catalytic nucleophile (36). Sts-1 and Sts-2 were originally described as negative regulators of T cell receptor (TCR) signaling pathways in T cells. Since then, their regulatory role in additional hematopoietic cell types, including platelets and mast cells, has been described (22, 23). As a wide range of leukocytes, including bone marrow-derived phagocytes and granulocytes, play a critical role during the initial primary immune response to *F. tularensis* (9, 12, 37), this study suggests the Sts proteins regulate immunological responses in a broader population of cells than previously appreciated. The enhanced restriction of *F. tularensis* in *Sts*<sup>-/-</sup> bone marrow-derived monocytes relative to wild-type bone marrow-derived monocytes following *ex vivo* infection supports this hypothesis. Freshly isolated bone marrow neutrophils lacking Sts expression also displayed reduced levels of *Francisella* growth *ex vivo*, relative to wild-type neutrophils. Given that neutrophils have been shown to support intracellular *Francisella* growth (34), it is possible that the Sts proteins regulate different functionally relevant pathways in neutrophils and monocytes.

The unique response of *Sts*<sup>-/-</sup> mice to *F. tularensis* infection has parallels to the response of *Sts*<sup>-/-</sup> mice to systemic infection by a very different pathogenic microorganism, the fungus *Candida albicans*. In a previous study, we reported that *Sts*<sup>-/-</sup> mice are profoundly resistant to disseminated candidiasis caused by bloodstream *C. albicans* infection. The major organ targeted in the mouse systemic *C. albicans* infection model is the kidney (38), and we observed a significant reduction in kidney fungal burden 24 h p.i. in *Sts*<sup>-/-</sup> mice relative to wild-type mice. This was accompanied by an absence of inflammatory lesions and significantly enhanced survival. Thus, in the context of infection by two widely different microbial pathogens, mice lacking Sts expression demonstrate beneficial responses and improved outcomes, including more rapid pathogen clearance. It is tempting to speculate that *in vivo* the Sts enzymes negatively regulate host inflammatory effector pathways that are important for eliminating diverse microbial agents. In such a scenario, we propose that their functional inactivation results in a distinct inflammatory environment that is uniquely suited to restricting microbial growth. However, given the enormous repertoire of different microbial pathogens and the many infectious conditions they elicit, it is most likely that Sts inactivation will differentially affect the host response to diverse microbial agents.

While mice lacking Sts expression demonstrate similarly overall positive outcomes to lethal systemic infection by both *F. tularensis* and *C. albicans*, we did observe a notable difference in their responses to the pathogens. For both organisms, widespread

pathogen dissemination following infections leads to multiple internal organs becoming infected. However, in the case of the *Sts*<sup>-/-</sup> mouse response to *C. albicans* infection, enhanced pathogen clearance was observed only within kidneys. In all other tissues examined, including the spleen, lung, liver, and brain, the rate of fungal clearance within organs lacking *Sts* expression was not substantively different from the rate of clearance in wild-type tissues (25). This stands in contrast to the manner in which *Sts*<sup>-/-</sup> mice respond to *F. tularensis* infection. In the latter case, enhanced bacterial clearance was manifested across a broader spectrum of tissues, including the lung, liver, and spleen. The underlying basis for the distinct pattern of pathogen-specific tissue restriction is unclear, although we surmise that different pathogens trigger distinct immunoregulatory cascades within different cells and tissues that may or may not be regulated by *Sts* activity.

The beneficial outcomes displayed by *Sts*<sup>-/-</sup> mice following lethal infection by two widely different microbial pathogens suggests the *Sts* enzymes could regulate a pathway(s) commonly used to control the immune response against different infectious microorganisms. To date, the *Sts* proteins have been established as negative regulators of receptor-proximal components of diverse signaling pathways. For example, within T cells, the *Sts* proteins target the important T cell kinase Zap-70 that is almost immediately downstream of TCR activation. Additionally, *Sts*-1 has been shown to control signaling downstream of both GPVI and Fc $\gamma$ RIIA in platelets and Fc $\epsilon$ RI in mast cells, by targeting the receptor-proximal Zap-70 homologue, Syk (22, 23). Syk has been shown to play an important role in the host response to *Francisella*. In particular, previous work has shown that Syk regulates phagocytosis and internalization of *Francisella* (39). However, we have not observed any differences in the internalization of LVS between wild-type and *Sts*<sup>-/-</sup> phagocytes. The intracellular pathways regulated by *Sts* during the response to intradermal *Francisella* infection are under investigation.

In the context of the *Sts*<sup>-/-</sup> response to *F. tularensis* infection, it is currently unclear which cells contribute to the enhanced resistance observed *in vivo* or which intracellular pathways are deregulated by the absence of *Sts*. Based on preliminary evidence, monocytic phagocytes are a leading cellular candidate. It is possible that *Sts*<sup>-/-</sup> monocytes recruited to peripheral tissues during the early stages of infection are the source of both the increased cytokine production and the enhanced bacterial restriction that are two hallmarks of the *Sts*<sup>-/-</sup> resistance phenotype. Neutrophils could also directly or indirectly contribute to enhanced protection, as *Sts*<sup>-/-</sup> mice both demonstrate increased neutrophil infiltration into the liver and spleen during the course of infection and demonstrate enhanced bacterial restriction *ex vivo*. Further investigation will be important in determining which cell types are the critical mediators of the increased resistance evident in *Sts*<sup>-/-</sup> mice.

Interestingly, inactivation of *Sts* was beneficial in the context of intradermal infection but not in the context of intranasal infection. It is known that the route of *Francisella* infection has a significant effect on the host immune response. In particular, it has been demonstrated that either neutrophil depletion or IFN- $\gamma$  neutralization renders mice more susceptible to intradermal infection but has a minimal effect on the outcome of a pulmonary infection (40). Thus, our results suggest the *Sts* proteins regulate functionally relevant pathways only in the context of specific infection scenarios.

As noted above, our model suggests that *Sts*-1 and *Sts*-2 negatively regulate an inflammatory signaling pathway(s) that controls innate immune responses against *F. tularensis* and *C. albicans*. In this model, *Sts* inactivation tips the balance of effector activation in such a way as to favor improved host cellular responses and enhanced microbial clearance. With respect to the dynamic relationship between host and pathogen, such a shift in activation levels might be most beneficial at early time points after infection, prior to the generation of widespread tissue damage that often occurs during an exuberant antimicrobial inflammatory response.

## MATERIALS AND METHODS

**Mice.** The generation of mice containing the Sts mutations, backcrossed 10 generations onto the C57/B6 background, has been described previously (41). Mice were housed and bred in the Stony Brook University Animal Facility under specific-pathogen-free conditions. Male mice used for the experiments were 6 to 8 weeks old. All mice were maintained in accordance with Stony Brook University Division of Laboratory Animal Resources (DLAR) guidelines. All animal experiments were approved by the Stony Brook University Institutional Animal Care and Use Committee (IACUC).

**Infections.** Wild-type *F. tularensis* LVS (ATCC 29684) bacteria were grown on chocolate II agar plates (Fisher) or overnight at 37°C in modified Mueller-Hinton broth (MHB) (containing 1% glucose, 0.025% ferric pyrophosphate, and 0.05% L-cysteine). Cultures were washed and resuspended in phosphate-buffered saline (PBS) to achieve the desired bacterial concentrations, and each mouse received a 100- $\mu$ l inoculum by intradermal injection. Inoculum levels were confirmed by plating serial dilutions onto chocolate agar plates after each infection. For intranasal infections, bacteria were grown as lawns on chocolate agar plates at 37°C 5% CO<sub>2</sub>. Bacteria were then washed and resuspended in MHB with 10% sucrose, and aliquots of the inoculum were frozen at -80°C. Bacterial counts of the prepared stocks were determined by serial plating. For infections, the inoculums were thawed and 20  $\mu$ l of the inoculum was administered to each mouse.

**Organ burden analysis.** Organs from mice sacrificed at days 2, 5, and 7 were harvested, weighed, and manually homogenized in stomacher bags in 1 ml PBS. Lysates were serially diluted and plated onto chocolate agar plates to determine the numbers of CFU. Bacterial burdens were calculated as CFU per gram of tissue.

**Generation of single-cell organ suspensions.** Spleens were manually crushed in PBS containing 2% fetal bovine serum (FBS) and filtered over a 70- $\mu$ m mesh, and leukocyte suspensions were treated with ACK lysis buffer (150 mM NH<sub>4</sub>Cl, 1 mM KHCO<sub>3</sub>, 0.1 mM EDTA) to lyse red blood cells (RBCs). Cells were resuspended in 2% FBS in PBS, in preparation for flow cytometric analysis. Liver and lung suspensions were prepared as described previously (25). Briefly, organs were dissociated in PBS plus 2% FBS and treated with 50 U/ml DNase (Roche) and 0.2 mg/ml Liberase TL enzyme (Roche) for 30 min at 37°C. Following erythrocyte lysis by the addition of ACK buffer, the debris was removed by straining and centrifugation, and the resulting pellet was suspended in PBS plus 2% FBS and centrifuged at 1,000  $\times$  g at room temperature over a 40% Ficoll cushion. The cell pellet was washed, filtered, and suspended in buffer for flow cytometric analysis.

**Flow cytometry.** Cell suspensions were incubated for 15 min with FC block prior to staining with fluorochrome-conjugated antibodies to the following for 30 min at 4°C: T cell receptor (TCR) (clone H57-597; BioLegend), CD19 (clone 6D5; BioLegend), NK1.1 (clone PK136; BioLegend), CD45 (clone 30-F11; BD Biosciences), Ly6C (clone AL-21; BioLegend), CD11c (clone N418; BD Biosciences), Ly6G (clone 1A8; BioLegend), F4/80 (clone BM8; BioLegend), CD11b (clone M1/70; BioLegend), CD115 (clone AFS98; BioLegend), CD80 (clone 16-10A1; BioLegend), CD86 (clone GL-1; BioLegend), CD4 (clone RM4-5; BD Biosciences), CD8 (clone 53-6-7; BD Biosciences), and I-A/I-E (clone M5/114.15.2; BioLegend). Prior to flow, splenocytes were treated with 7-aminoactinomycin D (7AAD; BioLegend). Flow cytometric data were acquired with a BD LSR Fortessa flow cytometer and analyzed with FlowJo software.

**Histology.** Spleens isolated from the uninfected or infected animals were fixed in buffered formalin. They were subsequently paraffin embedded and sectioned at 5  $\mu$ m by the Stony Brook University Histology Core staff. Sections were counterstained with hematoxylin and eosin (H&E).

**Cytokine analysis.** Spleens were homogenized in buffer containing 10 mM Tris (pH 7.8), 200 mM NaCl, 5 mM EDTA, and 10% glycerol with 1 $\times$  protease inhibitor cocktail (Roche). Clarified homogenates were analyzed for levels of indicated cytokines using a commercially available multiplex cytokine array (Millipore). Data were obtained and analyzed with a Bio-Plex 200 system (Bio-Rad).

**Preparations of cells for ex vivo infection assays.** Murine bone marrow-derived macrophages (BMDM) were obtained by isolating cells from the femurs of 6- to 8-week-old wild-type and *Sts*<sup>-/-</sup> mice and culturing them for 5 days as previously described (42). Briefly, cells were placed in bone marrow medium (BMM; Dulbecco's modified Eagle's medium [DMEM] with GlutaMax [Invitrogen], supplemented with 30% L929 cell supernatant, 20% FBS [Invitrogen], and 1 mM sodium pyruvate). On day 5, adherent cells were collected, suspended in BMM containing 15% L929 cell supernatant, 10% FBS, and 1 mM HEPES (pH 7.2), and cultured for 24 h prior to infection assays. Bone marrow-derived monocytes were obtained as described previously (33). Briefly, bone marrow cells were cultured for 4 days in medium as described above for BMDM, upon which nonadherent cells were collected and suspended in modified BMM (see above) in preparation for infection assays. Neutrophils were isolated by washing bone marrow cells in PBS containing 2% FBS and spinning them over a lymphoprep Ficoll gradient (Sigma) according to the manufacturer's instructions. The cell pellet was suspended in ACK lysis buffer to remove RBCs, pelleted, and resuspended in RPMI medium supplemented with 10% FBS prior to infection assays.

**Ex vivo infections.** BMDMs (1.5  $\times$  10<sup>5</sup>) were seeded in triplicate in 24-well plates and infected (multiplicity of infection [MOI], 50) with freshly grown *F. tularensis* LVS bacteria. Immediately following infection, cultures were gently spun (700 rpm, 5 min, room temperature) to facilitate contact between cells and bacteria. Plates were incubated with bacteria for 2 h, washed with PBS, and incubated for an additional 1 h with 50  $\mu$ g/ml gentamicin to kill extracellular bacteria. After antibiotic treatment, cells were washed with PBS and incubated with fresh medium (lacking gentamicin) at 37°C until the time points indicated in the figures. To assess counts of bacterial CFU, cells were lysed with 0.2% deoxycholic acid, lysates were serially diluted, and dilutions were plated onto chocolate agar plates for colony enumeration after 2 to 3 days of growth at 37°C. Bone marrow-derived monocytes (BMD-mo) (2  $\times$  10<sup>6</sup>) were seeded in triplicate in 24-well plates, stimulated with 100 ng/ml PMA for 2 h where specified, and

infected with *F. tularensis* LVS (MOI, 5). Plates were spun as described above, and the infection was allowed to proceed for 2 h, after which extracellular bacteria were eliminated by the addition of 50  $\mu\text{g/ml}$  gentamicin for 1 h. Cells were then collected, washed with PBS, suspended in antibiotic-free medium with or without 100 ng/ml PMA, and incubated for the indicated times. Bacterial CFU were determined as described above for BMDMs. Neutrophils ( $2 \times 10^6$  per well, triplicates) were treated and infected in the same way but did not receive any gentamicin treatment for the elimination of extracellular bacteria. After 24 h, bacterial enumeration was carried as described above.

**Cytotoxicity assays.** Culture supernatants were collected 24 h after *ex vivo* bacterial infection and analyzed for the presence of lactate dehydrogenase (LDH) using the CytoTox96 nonradioactive cytotoxicity assay (Promega) according to the manufacturer's instructions. Background LDH release was quantified by evaluating supernatants from uninfected cells, and maximum LDH was quantified from cells that were lysed by one freeze-thaw cycle. Percent LDH release was quantified by subtracting the background LDH release from all sample values, dividing by the maximum LDH release, and multiplying by 100.

**Ex vivo infections with virulent *F. tularensis* strain.** The *F. tularensis* subsp. *holarctica* KY99-3387 strain (from BEI Research Resources Repository, Manassas, VA) was cultivated on chocolate II agar plates (BD Biosciences) or in modified Mueller-Hinton broth (MHB [BD Biosciences] containing 1% glucose, 0.025% ferric pyrophosphate, and 0.05% L-cysteine HCl). All growth, manipulations, and cell culture infections of both fully virulent strains were performed under strict biosafety level 3 (BSL3) containment conditions at Stony Brook University. Monocyte infections were performed essentially as described above. BMD-mo ( $2 \times 10^6$ ) were seeded in triplicate in 24-well plates, stimulated with 100 ng/ml PMA for 2 h, and infected with strain KY99-3387 (MOI, 100). Plates were not centrifuged after the addition of bacteria, requiring the higher MOI. When necessary, cells were stimulated with both 100 ng/ml PMA and (50 ng/ml) IFN- $\gamma$  for 2 h prior to infection and again after the 1-h gentamicin step. Bacterial CFU counts were determined at the time points indicated in the figures.

## SUPPLEMENTAL MATERIAL

Supplemental material for this article may be found at <https://doi.org/10.1128/IAI.00406-17>.

**SUPPLEMENTAL FILE 1**, PDF file, 0.5 MB.

## ACKNOWLEDGMENTS

This work was supported by Stony Brook University, the Stony Brook Medical Center Dean's Office, funds from the National Institutes of Health, namely, grants R01AI080892 (N.C.) and R21AI115069 (D.G.T.), and funds from the G. Harold and Leila Y. Mathers Charitable Foundation (D.G.T.).

We thank Laurie Levine and the Stony Brook Department of Laboratory Animal Services for help with animal care, Todd Rueb and Rebecca Connor for help with fluorescence-activated cell sorter analysis, Dmitri Gnatenko for help with cytokine multiplex analysis, and Jeronimo Cello for assistance with BSL3 facilities. We also acknowledge the technical support provided by the Research Histology Core Laboratory, Department of Pathology, Stony Brook Medical Center. We thank Jorge Benach, Michael Hayman, and members of the Carpino and Thanassi laboratories for discussions. The following reagent was obtained through BEI Resources, NIAID, NIH: *Francisella tularensis* subsp. *holarctica*, strain KY99-3387, NR-647.

We declare no financial conflicts of interest.

## REFERENCES

- McLendon MK, Apicella MA, Allen LA. 2006. *Francisella tularensis*: taxonomy, genetics, and immunopathogenesis of a potential agent of biowarfare. *Annu Rev Microbiol* 60:167–185. <https://doi.org/10.1146/annurev.micro.60.080805.142126>.
- Asare R, Kwaik YA. 2010. Exploitation of host cell biology and evasion of immunity by *Francisella tularensis*. *Front Microbiol* 1:145. <https://doi.org/10.3389/fmicb.2010.00145>.
- Barel M, Charbit A. 2013. *Francisella tularensis* intracellular survival: to eat or to die. *Microbes Infect* 15:989–997. <https://doi.org/10.1016/j.micinf.2013.09.009>.
- Oyston PC. 2008. *Francisella tularensis*: unravelling the secrets of an intracellular pathogen. *J Med Microbiol* 57:921–930. <https://doi.org/10.1099/jmm.0.2008/000653-0>.
- Oyston PC, Sjostedt A, Titball RW. 2004. Tularemia: bioterrorism defense renews interest in *Francisella tularensis*. *Nat Rev Microbiol* 2:967–978. <https://doi.org/10.1038/nrmicro1045>.
- Bosio CM. 2011. The subversion of the immune system by *Francisella tularensis*. *Front Microbiol* 2:9. <https://doi.org/10.3389/fmicb.2011.00009>.
- Elkins KL, Cowley SC, Bosio CM. 2003. Innate and adaptive immune responses to an intracellular bacterium, *Francisella tularensis* live vaccine strain. *Microbes Infect* 5:135–142. [https://doi.org/10.1016/S1286-4579\(02\)00084-9](https://doi.org/10.1016/S1286-4579(02)00084-9).
- Conlan JW, Chen W, Bosio CM, Cowley SC, Elkins KL. 2011. Infection of mice with *Francisella* as an immunological model. *Curr Protoc Immunol* Chapter 19:Unit 19.14. <https://doi.org/10.1002/0471142735.im1914s93>.
- Periasamy S, Avram D, McCabe A, MacNamara KC, Sellati TJ, Harton JA. 2016. An immature myeloid/myeloid-suppressor cell response associated with necrotizing inflammation mediates lethal pulmonary tularemia. *PLoS Pathog* 12:e1005517. <https://doi.org/10.1371/journal.ppat.1005517>.
- Chong A, Celli J. 2010. The *Francisella* intracellular life cycle: toward molecular mechanisms of intracellular survival and proliferation. *Front Microbiol* 1:138. <https://doi.org/10.3389/fmicb.2010.00138>.

11. Brunton J, Steele S, Miller C, Lovullo E, Taft-Benz S, Kawula T. 2015. Identifying *Francisella tularensis* genes required for growth in host cells. *Infect Immun* 83:3015–3025. <https://doi.org/10.1128/IAI.00004-15>.
12. Gillette DD, Tridandapani S, Butchar JP. 2014. Monocyte/macrophage inflammatory response pathways to combat *Francisella* infection: possible therapeutic targets? *Front Cell Infect Microbiol* 4:18. <https://doi.org/10.3389/fcimb.2014.00018>.
13. Cowley SC, Elkins KL. 2011. Immunity to *Francisella*. *Front Microbiol* 2:26. <https://doi.org/10.3389/fmicb.2011.00026>.
14. McCracken JM, Kinkead LC, McCaffrey RL, Allen LA. 2016. *Francisella tularensis* modulates a distinct subset of regulatory factors and sustains mitochondrial integrity to impair human neutrophil apoptosis. *J Innate Immun* 8:299–313. <https://doi.org/10.1159/000443882>.
15. Henry T, Monack DM. 2007. Activation of the inflammasome upon *Francisella tularensis* infection: interplay of innate immune pathways and virulence factors. *Cell Microbiol* 9:2543–2551. <https://doi.org/10.1111/j.1462-5822.2007.01022.x>.
16. Fernandes-Alnemri T, Yu JW, Juliana C, Solorzano L, Kang S, Wu J, Datta P, McCormick M, Huang L, McDermott E, Eisenlohr L, Landel CP, Alnemri ES. 2010. The AIM2 inflammasome is critical for innate immunity to *Francisella tularensis*. *Nat Immunol* 11:385–393. <https://doi.org/10.1038/ni.1859>.
17. Jones JW, Kayagaki N, Broz P, Henry T, Newton K, O'Rourke K, Chan S, Dong J, Qu Y, Roose-Girma M, Dixit VM, Monack DM. 2010. Absent in melanoma 2 is required for innate immune recognition of *Francisella tularensis*. *Proc Natl Acad Sci U S A* 107:9771–9776. <https://doi.org/10.1073/pnas.1003738107>.
18. Fitzgerald KA, Rathinam VA. 2015. GBPs take AIM at *Francisella*. *Nat Immunol* 16:443–444. <https://doi.org/10.1038/ni.3144>.
19. Man SM, Karki R, Sasai M, Place DE, Kesavardhana S, Temirov J, Frase S, Zhu Q, Malireddi RK, Kuriakose T, Peters JL, Neale G, Brown SA, Yamamoto M, Kanneganti TD. 2016. IRGB10 liberates bacterial ligands for sensing by the AIM2 and caspase-11-NLRP3 inflammasomes. *Cell* 167:382–396. <https://doi.org/10.1016/j.cell.2016.09.012>.
20. Tsygankov AY. 2013. TULA-family proteins: a new class of cellular regulators. *J Cell Physiol* 228:43–49. <https://doi.org/10.1002/jcp.24128>.
21. Carpino N, Turner S, Mekala D, Takahashi Y, Zang H, Geiger TL, Doherty P, Ihle JN. 2004. Regulation of ZAP-70 activation and TCR signaling by two related proteins, Sts-1 and Sts-2. *Immunity* 20:37–46. [https://doi.org/10.1016/S1074-7613\(03\)00351-0](https://doi.org/10.1016/S1074-7613(03)00351-0).
22. Thomas DH, Getz TM, Newman TN, Dangelmaier CA, Carpino N, Kunapuli SP, Tsygankov AY, Daniel JL. 2010. A novel histidine tyrosine phosphatase, TULA-2, associates with Syk and negatively regulates GPVI signaling in platelets. *Blood* 116:2570–2578. <https://doi.org/10.1182/blood-2010-02-268136>.
23. de Castro RO, Zhang J, Groves JR, Barbu EA, Siraganian RP. 2012. Once phosphorylated, tyrosines in carboxyl terminus of protein-tyrosine kinase Syk interact with signaling proteins, including TULA-2, a negative regulator of mast cell degranulation. *J Biol Chem* 287:8194–8204. <https://doi.org/10.1074/jbc.M111.326850>.
24. Reppschlagel K, Gosselin J, Dangelmaier CA, Thomas DH, Carpino N, McKenzie SE, Kunapuli SP, Tsygankov AY. 2016. TULA-2 protein phosphatase suppresses activation of Syk through the GPVI platelet receptor for collagen by dephosphorylating Tyr(P)346, a regulatory site of Syk. *J Biol Chem* 291:22427–22441. <https://doi.org/10.1074/jbc.M116.743732>.
25. Naseem S, Frank D, Konopka JB, Carpino N. 2015. Protection from systemic *Candida albicans* infection by inactivation of the Sts phosphatases. *Infect Immun* 83:637–645. <https://doi.org/10.1128/IAI.02789-14>.
26. Fortier AH, Slayter MV, Ziemba R, Meltzer MS, Nacy CA. 1991. Live vaccine strain of *Francisella tularensis*: infection and immunity in mice. *Infect Immun* 59:2922–2928.
27. Chiavolini D, Alroy J, King CA, Jorth P, Weir S, Madico G, Murphy JR, Wetzler LM. 2008. Identification of immunologic and pathologic parameters of death versus survival in respiratory tularemia. *Infect Immun* 76:486–496. <https://doi.org/10.1128/IAI.00862-07>.
28. Kirimanjeswara GS, Olmos S, Bakshi CS, Metzger DW. 2008. Humoral and cell-mediated immunity to the intracellular pathogen *Francisella tularensis*. *Immunol Rev* 225:244–255. <https://doi.org/10.1111/j.1600-065X.2008.00689.x>.
29. Malik M, Bakshi CS, McCabe K, Catlett SV, Shah A, Singh R, Jackson PL, Gaggari A, Metzger DW, Melendez JA, Blalock JE, Sellati TJ. 2007. Matrix metalloproteinase 9 activity enhances host susceptibility to pulmonary infection with type A and B strains of *Francisella tularensis*. *J Immunol* 178:1013–1020. <https://doi.org/10.4049/jimmunol.178.2.1013>.
30. Allen LA. 2013. Editorial: leukocytes in tularemia—so many cells, so little time. *J Leukocyte Biol* 93:641–644. <https://doi.org/10.1189/jlb.1212661>.
31. Woolard MD, Frelinger JA. 2008. Outsmarting the host: bacteria modulating the immune response. *Immunol Res* 41:188–202. <https://doi.org/10.1007/s12026-008-8021-5>.
32. Steiner DJ, Furuya Y, Metzger DW. 2014. Host-pathogen interactions and immune evasion strategies in *Francisella tularensis* pathogenicity. *Infect Drug Resist* 7:239–251. <https://doi.org/10.2147/IDR.S53700>.
33. Francke A, Herold J, Weinert S, Strasser RH, Braun-Dullaeus RC. 2011. Generation of mature murine monocytes from heterogeneous bone marrow and description of their properties. *J Histochem Cytochem* 59:813–825. <https://doi.org/10.1369/0022155411416007>.
34. McCaffrey RL, Allen LA. 2006. *Francisella tularensis* LVS evades killing by human neutrophils via inhibition of the respiratory burst and phagosome escape. *J Leukocyte Biol* 80:1224–1230. <https://doi.org/10.1189/jlb.0406287>.
35. McCaffrey RL, Schwartz JT, Lindemann SR, Moreland JG, Buchan BW, Jones BD, Allen LA. 2010. Multiple mechanisms of NADPH oxidase inhibition by type A and type B *Francisella tularensis*. *J Leukocyte Biol* 88:791–805. <https://doi.org/10.1189/jlb.1209811>.
36. Rigden DJ. 2008. The histidine phosphatase superfamily: structure and function. *Biochem J* 409:333–348. <https://doi.org/10.1042/BJ20071097>.
37. Rasmussen JW, Tam JW, Okan NA, Mena P, Furie MB, Thanassi DG, Benach JL, van der Velden AW. 2012. Phenotypic, morphological, and functional heterogeneity of splenic immature myeloid cells in the host response to tularemia. *Infect Immun* 80:2371–2381. <https://doi.org/10.1128/IAI.00365-12>.
38. Lionakis MS, Lim JK, Lee CC, Murphy PM. 2011. Organ-specific innate immune responses in a mouse model of invasive candidiasis. *J Innate Immun* 3:180–199. <https://doi.org/10.1159/000321157>.
39. Parsa KVL, Butchar JP, Rajaram MVS, Cremer TJ, Tridandapani S. 2008. The tyrosine kinase Syk promotes phagocytosis of *Francisella* through the activation of Erk. *Mol Immunol* 45:3012–3021. <https://doi.org/10.1016/j.molimm.2008.01.011>.
40. Conlan JW, Kuo Lee R, Shen H, Webb A. 2002. Different host defenses are required to protect mice from primary systemic vs pulmonary infection with the facultative intracellular bacterial pathogen *Francisella tularensis* LVS. *Microb Pathog* 32:127–134. <https://doi.org/10.1006/mpat.2001.0489>.
41. San Luis B, Sondgeroth B, Nassar N, Carpino N. 2011. Sts-2 is a phosphatase that negatively regulates zeta-associated protein (ZAP)-70 and T cell receptor signaling pathways. *J Biol Chem* 286:15943–15954. <https://doi.org/10.1074/jbc.M110.177634>.
42. Doyle CR, Pan JA, Mena P, Zong WX, Thanassi DG. 2014. TollC-dependent modulation of host cell death by the *Francisella tularensis* live vaccine strain. *Infect Immun* 82:2068–2078. <https://doi.org/10.1128/IAI.00044-14>.